Geogr. Fis. Dinam. Quat.
37 (2014), 113-130, 24 figg., 1 tab.

DOI 10.4461/GFDQ.2014.37.11

NICOLA SCIARRA (*), DARIA MARCHETTI (**), GIACOMO D'AMATO AVANZI (**) & MONIA CALISTA (*)

ROCK SLOPE ANALYSIS ON THE COMPLEX LIVORNO COASTAL CLIFF (TUSCANY, ITALY)

ABSTRACT: SCIARRA N., MARCHETTI D., D'AMATO AVANZI G. & CALISTA M., *Rock slope analysis on the complex Livorno coastal cliff (Tuscany, Italy).* (IT ISSN 0391-9838, 2014).

The landscape of the south coast of Livorno city (Tuscany, Italy) is characterized by sandstone headlands and sandy pocket beaches affected by serious stability problems. Lithological features and physical-chemical processes involve many slope failures concerning the sandstone cliff and extending all over the cliff height; these failures often threaten people and facilities. The most prominent positive relief landform is structurally controlled by three main closely spaced joint sets. The presence of leaning and collapsed rock blocks suggests that erosion and mass wasting maintain the cliff steepness and elevate risk conditions. The sandstone mechanical properties and discontinuity pattern have been investigated in order to determine the response of the rock mass to subaerial and marine stresses. The sandstone outcrops were characterized according to the Rock Mass Rating (Bieniawski, 1989) and the Slope Mass Rating (Romana, 1985; 1993). Such data has been reported in a GIS system in order to determine the landslide susceptibility of the cliff. Some numerical modelling, with a code at Distinct Element Method model, were carried out to evaluate stresses and displacement distribution near the free surface of a steep slope face, as a function of steepness, dip direction and rock mass quality. Then some fall simulations were carried out, to make a back analysis of previous events and to obtain a more general outline of possible movements. The results showed that rock mechanics and computer modelling can be effective tools in predicting the rock-mass stability, determining the mechanism by which blocks fall from steep slopes and their possible trajectories.

KEY WORDS: Rock mass, Rock fall, RMR, SMR, Distinct Element Method, Coast of Livorno, Italy.

RIASSUNTO: SCIARRA N., MARCHETTI D., D'AMATO AVANZI G. & CALISTA M., *Analisi di stabilità in roccia lungo la falesia costiera di Livorno (Toscana, Italia).* (IT ISSN 0391-9838, 2014).

Il paesaggio della costa meridionale di Livorno (Toscana, Italia) è caratterizzato da promontori di arenaria e piccole spiagge sabbiose affetti da gravi problemi di stabilità. Le caratteristiche litologiche dei luoghi ed i processi chimico-fisici in atto hanno determinato numerosi fenomeni di rottura nei versanti estendendo le problematiche anche più a monte; tali crolli causano gravi problemi di utilizzo delle aeree. Il più importante rilievo morfologico è strutturalmente controllato da tre principali e ravvicinati set di giunti di discontinuità. La presenza di blocchi di roccia sia in stato di crollo imminente sia già crollati suggerisce che le condizioni erosive e le perdite di massa contribuiscano a mantenere la falesia in condizioni di elevata pendenza e di rischio molto elevato. Le proprietà meccaniche dell'ammasso lapideo ed il modello di discontinuità sono stati studiati al fine di determinare la risposta dell'ammasso agli stress subaerei e marini. Gli affioramenti di arenaria sono stati caratterizzati secondo il criterio RMR di Bieniawski (1989) ed SMR di Romana (1985, 1993). Tutti i dati sono stati riportati in un sistema GIS al fine di determinare la suscettibilità da frana della falesia. Alcune modellazioni numeriche, eseguite con un codice di calcolo agli Elementi Distinti, sono state compiute per valutare la distribuzione delle sollecitazioni ed i probabili spostamenti in prossimità della superficie libera del versante, in funzione della pendenza, delle caratteristiche di discontinuità e della qualità della massa rocciosa. Inoltre, sono state effettuate alcune simulazioni di crollo, per studi di back analysis, confrontando i risultati con eventi precedentemente accaduti al fine di ottenere un quadro più generale dei possibili movimenti futuri. I risultati hanno evidenziato una ottima corrispondenza tra gli studi di meccanica delle rocce ed i modelli numerici implementati, fornendo insieme uno strumento combinato efficace per prevedere la stabilità dell'ammasso e per determinare il meccanismo con cui i blocchi cadono e le loro possibili traiettorie.

TERMINI CHIAVE: Ammasso roccioso, Crollo di roccia, RMR, SMR, Metodo agli Elementi Distinti, Costa di Livorno, Italia.

INTRODUCTION

The coast south of Livorno, along the Ligurian Sea, shows predominant rocky shores and cliffs, while beaches are small and rare. The coast section between Calafuria and Sassoscritto headlands (fig. 1) is appreciated by tourists and bathers, because of its wonderful landscape (fig. 2), with windswept promontories and quiet coves, where the Libeccio wind (a violent south-westerly wind) causes spectacular and picturesque sea storms (fig. 3). Therefore, chiefly in the summertime many people frequent this area. Unfortunately, this coast hides some dan-

(*) *Dipartimento di Ingegneria e Geologia, Università di Chieti-Pescara, Italy.*

(**) *Dipartimento di Scienze della Terra, Università di Pisa, Italy.*

FIG. 1 - Aerial view of the study area (image from Google Earth).

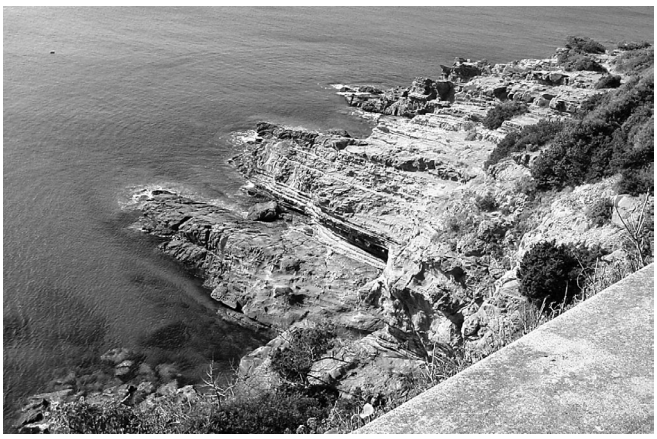

FIG. 2 - A rocky shore in the study area.

FIG. 3 - A sea storm at Calafuria. The main road Aurelia and the railway are visible to the right (photo Marco Lorusso, LaMMA).

gers, due to sudden and rapid rock falls, which threaten the sea shore and its access ways (fig. 4).

This paper, following a preliminary paper of Marchetti & *alii* (2008), particularly focuses on the coast of Calafuria-Sassoscritto, between the mouth of Rio Maroccone to the north-west and the Cala del Leone to the south-east. The preliminary paper considered the main dangerous area, between the sea and the main road Aurelia and aimed at assessing the landslide hazard and modelling instability initiation and evolution.

FIG. 4 - Bathers close to a rock fall accumulation.

GEOLOGICAL SETTING

In the study area few tectonic units crop out. They originated from different paleogeographic domains of the Northern Apennines (from west to east: Ligurian Domain, Sub-Ligurian Domain, and Tuscan Domain). The Tuscan Nappe (Tuscan Domain) is the most widespread unit in Tuscany (Carmignani & *alii*, 2004) and includes several formations ranging in age from Upper Triassic to Lower Miocene: among them the Macigno Fm. (Upper Oligocene-Lower Miocene) constitutes the studied coast (fig. 5). Ligurian and Sub-Ligurian units border the study area. Pleistocene-Holocene deposits are also present, due to fluvial, slope and marine processes.

The Macigno Fm. consists of mostly medium- to thick-bedded siliciclastic turbidites made of grey-brown sandstone (Pandeli & *alii*, 1994) and was named Arenaceous Flysch of Calafuria by Lazzarotto & *alii* (1990), as a lateral sediment easterly of the most typical Apenninic Macigno. It is well exposed at Calafuria and Sassoscritto (fig. 6) and all along the cliff, where it shows high to very high sandstone/shale ratio and predominant thick or very thick, coarse - to very coarse-grained beds. The sandstone is mainly composed of quartz, feldspar and mica, with high percentage of carbonate cement (Ferrini & *alii*, 1995). The depositional environment is mainly referable to channelled

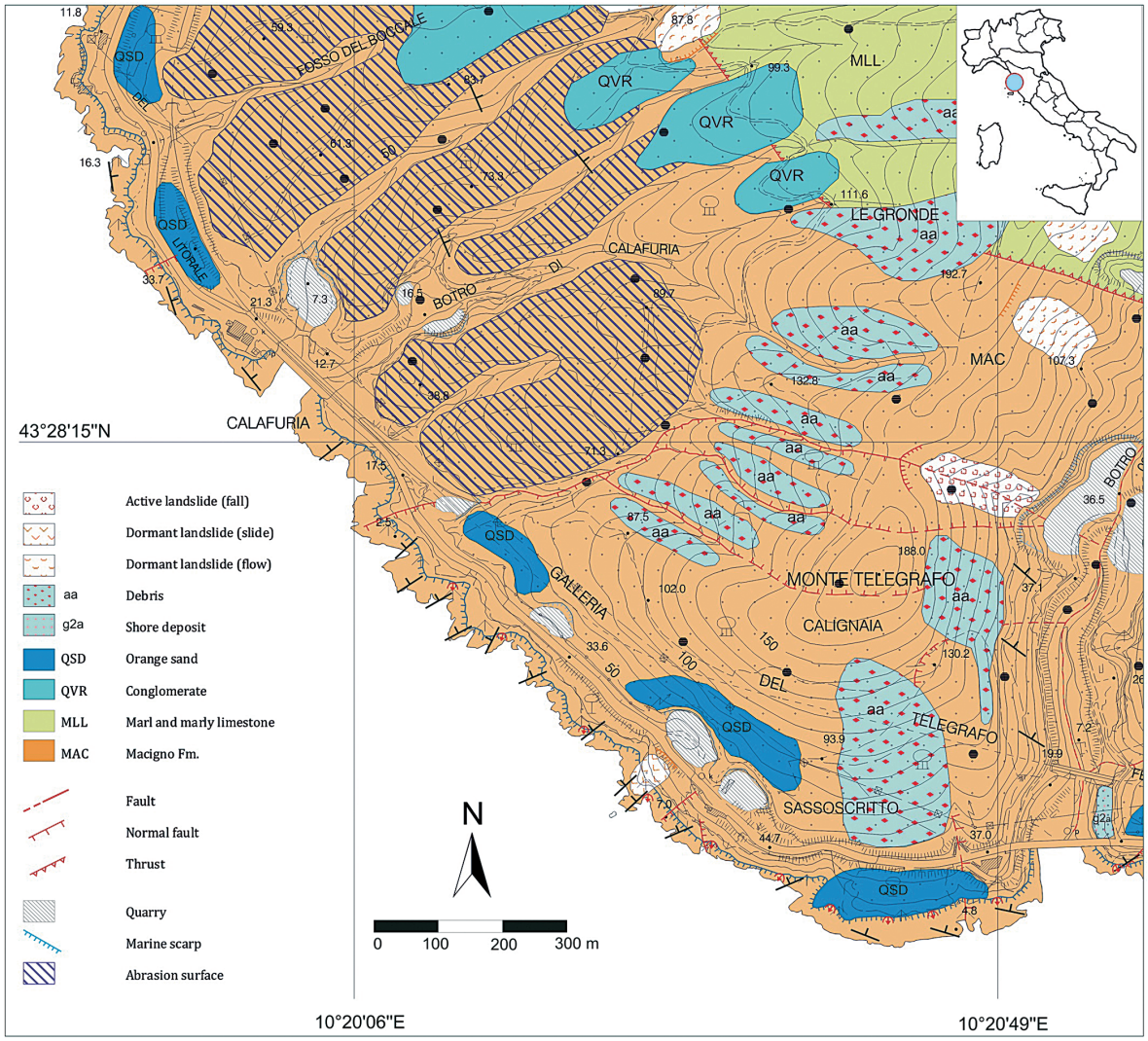

FIG. 5 - Geologic map of the study area.

submarine fans (Pandeli & *alii*, 1994). Although the Bouma (1962) sequence may be complete, the massive interval prevails; thick and coarse facies and amalgamation of beds are frequent.

Peculiar alveolar erosion (fig. 6) characterizes the area of Sassoscritto (the toponym means «Written Stone»). It is probably due to the combined action of the salt and wind.

The structural geological pattern results from a multiphase compressional and tensional deformation of the Northern Apennines between the Upper Cretaceous and the Lower Pliocene (Elter & *alii*, 1975; Conti & *alii*, 2004). Folds, joints and faults testify this evolution in the study area. The Macigno Fm. show a mainly monocline structure, NW-SE trending and dipping 20-30° into the slope. Along the coast line, bedding may be oblique to the slope direction. Faults show three main directions: NW-SE (Apenninic, normal faults), NS (normal faults) and NE-SW (Anti-Apenninic, transfer faults). Among them, the Mt. Tele-

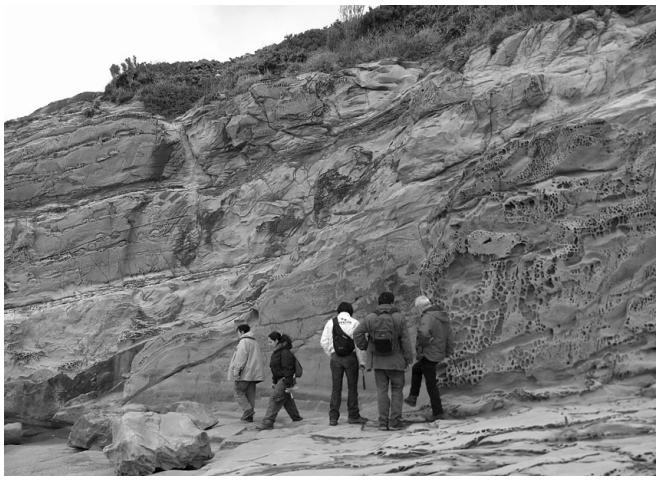

FIG. 6 - The Macigno Fm. is well exposed at Sassocritto. The alveolar erosion visible on the right gives the site the local name «Sassoscritto» (meaning «written stone»).

grafo fault system displaces large fault blocks between Calafuria and Cala del Leone. Therefore joint sets and bedding show variable arrangements: as it will be explained later, this variability greatly influences rock mass properties and slope stability.

Structural pattern of the Macigno Fm.

The structural features of the Macigno Fm. based on site surveys and stereographic analysis (Wulff projection) are depicted and synthesized in fig. 7. The contour plots of the discontinuities are represented; 3 median poles, corresponding to 3 median planes were identified. They may be assumed to be representative of 3 families of discontinuities (bedding and two joint sets), characterized by the following values of dip direction/dip. They are listed in order of decreasing frequency:

– 320/24 (bedding)
– 190/70 (joint set)
– 250/80 (joint set)

Morphological outline

The present landscape results from several different processes, referable to the tectonics and to the action of gravity, climate, running water, waves and tides, winds, and man.

The investigated cliff is mainly part of a hillside slope, which has a triangular shape and is densely covered by vegetation (Mediterranean *maquis* and wood). The highest elevation is modest (about 200 m a.s.l.), while on average the slope inclination is about 10° (18%). Along the southeast and west slopes of the Mt. Telegrafo the steepness increases up to about 30-35° (58-70%). Very high slope gradients are found in quarries and along the seashore cliff.

From north to south few streams drain the hill: the Maroccone, the Calafuria and the Calignaia torrents, whose lengths are shorter than 2-3 km. Their discharge is normally moderate, or absent in dry periods. Heavy rainfalls can cause flash floods.

The coast shows a sequence of coves and headlands, creating an indented coastline, structurally controlled by

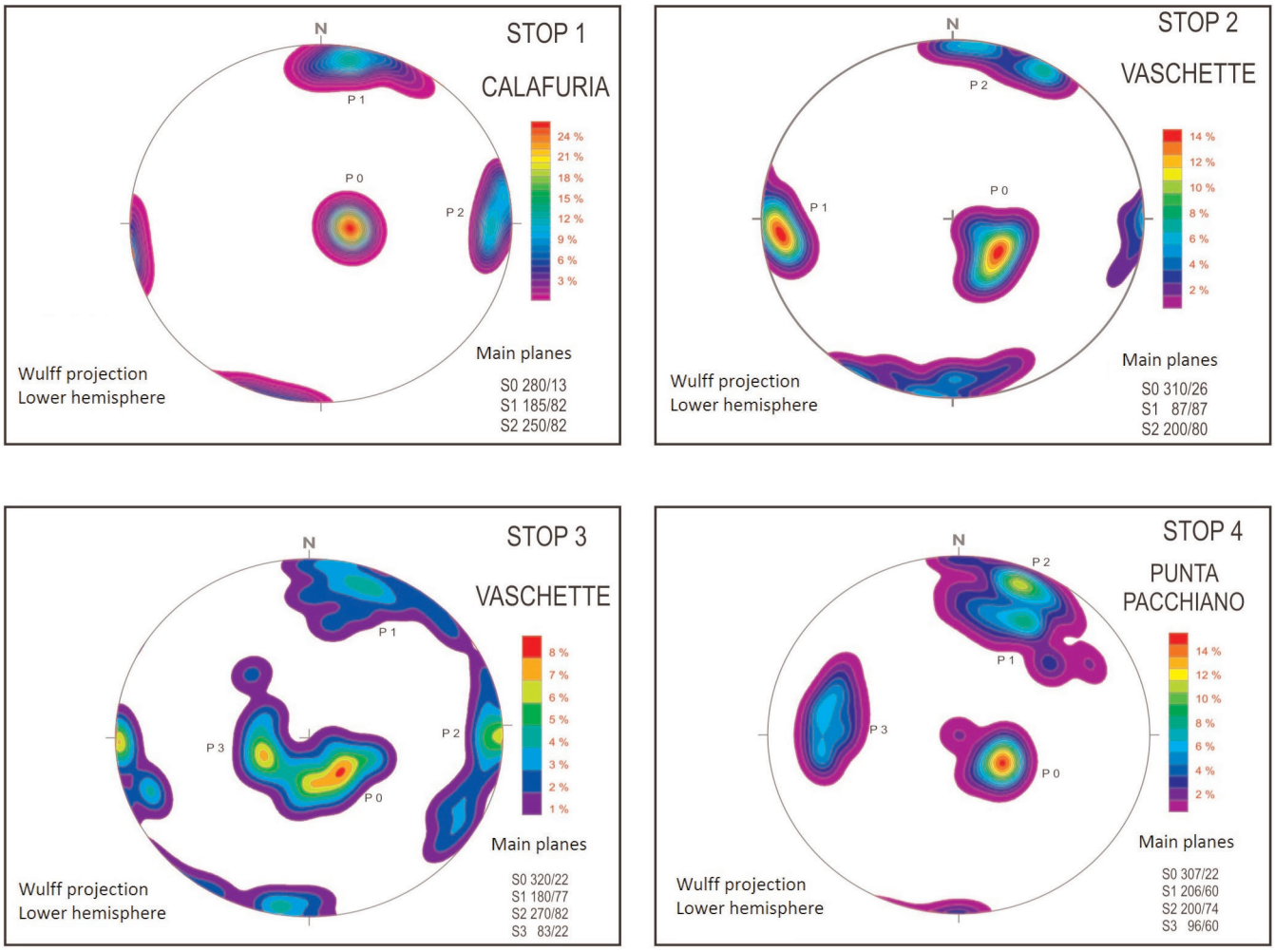

FIG. 7 - Structural pattern of the Macigno Fm.

joints and bedding (see figs. 1 and 2). Steep rocky cliffs prevail and often hang over the shoreline.

The anthropogenic morphology is mostly referable to the main road Aurelia, to the railway and to quarrying. The construction of the Aurelia and the coastal railway mainly goes back to the XIX-XX century. In time this implied excavation of slopes, opening of quarries, realization of tunnels and viaducts and widening of the roadway. Hence some stability problems likely occurred.

Galoppini & *alii* (1995-1996) report several quarries of sandstone in the study area. All of them are referable to the industrial age and now are inactive. The large quarries are clearly visible on the aerial view of fig. 1. They are close to the road, except the bigger one, which is along the Calignaia stream valley. Most of them show an amphitheatre shape and dense reforestation.

Small quarries go back to the preindustrial and to the Etruscan-Roman ages. They are close to the coast and often face the see and several are hidden by the vegetation. Nevertheless, some quarries along the shore are still visible. They belong to the Etruscan-Roman age and at present are below the sea level. Polygonal excavations constitute small pools, very appreciated by bathers (fig. 8). This submersion is probably due to eustatic changes in sea level and/or to tectonic movements. They are evidences of the work of ancient peoples and can be regarded as a historical and geological heritage.

Seismicity

It should be mentioned that recurrent earthquakes hit the study area. In the last centuries, four VII MCS (1646, 1742, 1771 and 1714) and one IX MCS / 5.7 M (14/8/1846) earthquakes occurred around Livorno. In the last ten years, some significant events have been recorded, with a Magnitude up to 4.1 (Regione Toscana - Seismic Risk, web site).

FIG. 8 - An ancient (Roman-Etruscan) submerged quarry along the rock shore. Polygonal excavations are evident.

According to the Tuscany Region Seismic Classification (2012), the study area falls into the 3th seismic zone, where the peak ground acceleration a_g is ≤ 0.150 g and g is the gravity acceleration (Regione Toscana - Seismic Risk, web site).

Earthquakes can affect slope stability. Therefore they will be considered in the stability modelling of the cliff, using a cautionary acceleration $a_g = 0.25$g.

GEOMECHANICAL OBSERVATIONS

A geotechnical study was carried out on the Macigno Fm. on site. Field surveys and indirect tests for classifying the rock masses and to estimate the uniaxial compressive strength were performed in situ with the Schmidt hammer and in the laboratory with the point load test.

UNIAXIAL COMPRESSIVE STRENGTH (UCS)

In the study area, a type-L Schmidt hammer (impact energy of 0.735 Nm) was used. Various empirical equations have been proposed for estimating UCS from the Schmidt hammer rebound number (such as Deer & Miller (1966), Katz & *alii* (2000), Yasar & Erdogan (2004), Aydin & Basu (2005), Fener & *alii* (2005). In the study area the analyses were based on the well-known and commonly used Deer & Miller (1966) relation, which allows easy comparison of the results. In order to estimate the UCS, it considers the hammer rebound, impact direction and the unit weight of the rock.

The point load test, being basically a splitting test, needs to establish a relation between point load index and UCS and different studies have proposed different relations. Lacking any direct UCS determination, the procedure and relation proposed by Broch & Franklin (1972) and ISRM (1981) were used. They suggest that the UCS is about 24 times the point load index, referred to a standard size of 50 mm. In the definition of the UCS of the intact rock, an important index for the geomechanical classification, the values from the point load test are considered more reliable than those gathered from the Schmidt Hammer, since the point load test suffers from the fracturing of the rock mass less than the other instrument. Two representative domains of rock strength derive from the frequency distribution of Is(50) values obtained for the various samples (fig. 9).

These sets are represented by modal values of the Is(50) equal to 1.7 MPa and 3.0 MPa, related respectively to samples with medium/coarse grain and fine grain; from these values the UCS of the intact rock respectively results equal to 41 MPa and 72 MPa. According to the ISRM classification, the strength is moderately low in the coarse-grained samples and moderately high in the fine-grained samples.

GEOMECHANICAL CLASSIFICATIONS OF UNSTABLE ROCK MASSES

Rock masses were analysed according to the Bieniawski's RMR and the Romana's SRM classifications, commonly used in the world.

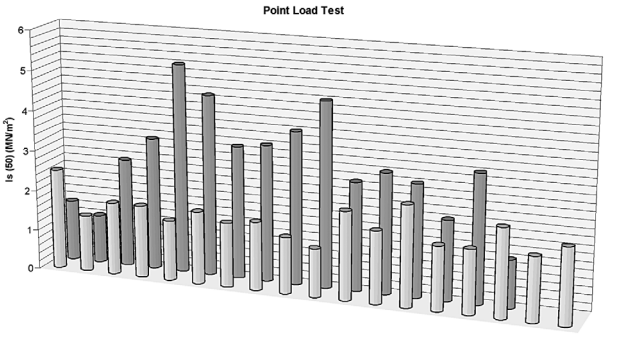

	1	2	3	4	5	6	7	8	9	10	11	12	13	14	15	16	17	18
Medium/coarse grained	2,5	1,4	1,8	1,8	1,5	1,8	1,6	1,7	1,4	1,2	2,2	1,8	2,5	1,6	1,6	2,2	1,6	1,9
Fine grained	1,5	1,2	2,7	3,3	5,2	4,5	3,3	3,4	3,8	4,6	2,7	3	2,8	2	3,2	1,2		

FIG. 9 - Two representative domains of Is(50) resulting from the Point Load Test.

Rock Mass Rating (RMR)

In order to obtain a preliminary assessment of the rock mass instability, the Rock Mass Rating (RMR; Bieniawski, 1989) was applied to the rocky wall. The RMR considers and rates some key parameters: intact rock strength, rock quality designation (RQD), spacing of discontinuities, conditions of discontinuities (persistence, separation, roughness, infilling, and weathering), groundwater conditions, and discontinuity orientation vs. slope. The basic RMR (RMR_B) may be obtained from the normal RMR, without adjusting for the discontinuity orientation vs. slope orientation. The RMR_B can better describe the rock mass properties and can be a very useful tool in evaluating geomechanical parameters of a rock mass, such as cohesion and friction angle.

In the coastal area, the Macigno Fm. was subdivided into two zones with different geomechanical qualities:

Zone 1- III class (RMR_B = 54): sandstone.

– This lithofacies is well represented in the area. It shows a structural pattern with regular bedding, with layers up to 30 cm thick. It has a medium UCS value (modal value of 72 MPa), with moderately to widely spaced discontinuities; the conditions of the discontinuities vary from closed and dry to open and filled with incoherent material.

Zone 2 - IV class (RMR_B = 36): sandstone.

– This lithofacies differs from the other previous for a coarser grain; it shows a lower UCS and the discontinuity conditions are slightly poorer.

To explain the stability conditions of the study area, it was considered necessary, once the geomechanical features were defined, to analyse the relationship between slope and joints attitudes, for identifying unstable rock blocks and movements that may occur also in static conditions. Afterwards it could be possible to consider induced loads, like water pressure or seismic loads. The most critical areas for boulders and / or wedges detachment, as will be discussed in the following paragraph, were identified by evaluating the stability of rock slopes, according to the SMR classification proposed by Romana (1985; 1993). That classification, arisen from the RMR Index, considers the relationship between discontinuities and slope.

Slope Mass Rating (SMR)

The Slope Mass Rating (SMR; Romana 1985, 1993) is obtained from the RMR_B by adding an adjustment factor depending on the relative orientation of joints ($\alpha j;\beta j$) and slope ($\alpha s;\beta s$) and another adjustment factor depending on the method of excavation:

$SMR = RMR_B + (F1 \times F2 \times F3) + F4$.

With the use of a GIS platform it has been possible to determine the areal changes of the SMR. A DEM (Digital Elevation Model) was carried out according to the digital mapping, then it was transformed into a grid whose cells (pixels) are 1 meter in length. The digital models «Slope» and «Aspect» were derived from it: they allow to display the characteristics of slope and exposure of the area respectively.

Two RMR maps were carried out for each discontinuity family: the first represents the planar slide susceptibility and the other represents the toppling susceptibility. This result was obtained through several operations executed on the attributes tables of the corresponding layers. These steps are briefly described here:

- the value of F1 parameter for planar slide and toppling, as defined by the Romana's RMR classification ($|\alpha j - \alpha s|$ and $|\alpha j - \alpha s - 180°|$) was derived from the «Aspect» database (αs) and from the dip direction values of each of the three joint sets (αj). Then it was converted to the obtained values in indices on the basis of the categories proposed by Romana;
- the parameter F2 is βj, therefore it is a constant value for each family;
- the values of F3 were derived from the «Slope» values (β_S) and from the dip of the three families (βj): in the case of planar sliding it was obtained through the difference $\beta j - \beta_S$, while in the case of toppling it was obtained through the sum $\beta j + \beta_S$; then it was converted to the obtained values in indices on the basis of the categories proposed by Romana;
- the value of the F4 parameter, because they are natural slopes, was considered «+15» in all cases.

The identification of areas with higher probability of landslides movements has been achieved through the overlaying of different layers, each of which corresponds to the Romana classification factors (F1, F2, F3, F4). The following considerations arise from the maps:

- Planar sliding - Joint set A (320/24): the F1 factor is critical where the slope is N/NW facing (because the planar sliding is more likely where joints and slope dip directions are similar). The F3 factor is critical in many areas because this set has got a low dip value, so the situation «dipping downslope» is very frequent. However the planar sliding map shows that the rock mass stability is mostly controlled by the basic RMR.

- Planar sliding - Joint set B (190/70): this set is south facing, then F1 will be high where the slope has similar dip direction; the value of dip of these discontinuities is rather high (70°) then there will be critical conditions where the slope steeply dips towards the sea. Again, the planar sliding map shows that the rock mass stability is mostly controlled by the basic RMR.
- Planar sliding - Joint set C (250/80): joints belonging to the C family are W-SW facing, so the F1 values will be critical in the slopes with similar dip direction; in this case F3 is less relevant than in the previous case because the dip is even higher (80°)
- Toppling - Joint set A: F1 is critical where the slope is SE facing. The dip of these joints is very low so there is very low toppling probability, in fact F3 is everywhere equal to zero.
- Toppling - Joint set B: the F1 value is low throughout the study area because there aren't North facing slopes. F3 reaches critical values where there are slopes ≥ 50° steep.
- Toppling - Joint set C: F1 is critical where slopes are E-NE facing (only in a small area north of the Calignaia bridge). For F3 the same observations made for the family B are applied. These two factors affect the slope stability, but it is generally governed by the geomechanical quality of the Macigno Fm.

It is clear that the stability of the rock mass that constitute the Romito cliff is linked to the quality of the rock mass (and therefore of the structural domain in which it falls) rather than to the relationship between joints and slope attitudes.

These observations were summarized in a map of areas with SMR index <40, shown in fig. 10. The RMR classification provides a high probability of all types of movements, planar sliding, wedge sliding or toppling, where the index is less than this value.

Numerical modelling

After geomechanical surveys some numerical analyses were performed on two particularly interesting sections (fig. 11), using a two-dimensional Universal Distinct Element Method code (UDEC 4.0, 2004). It simulates the response of a discontinuous, as a jointed rock mass, subject-

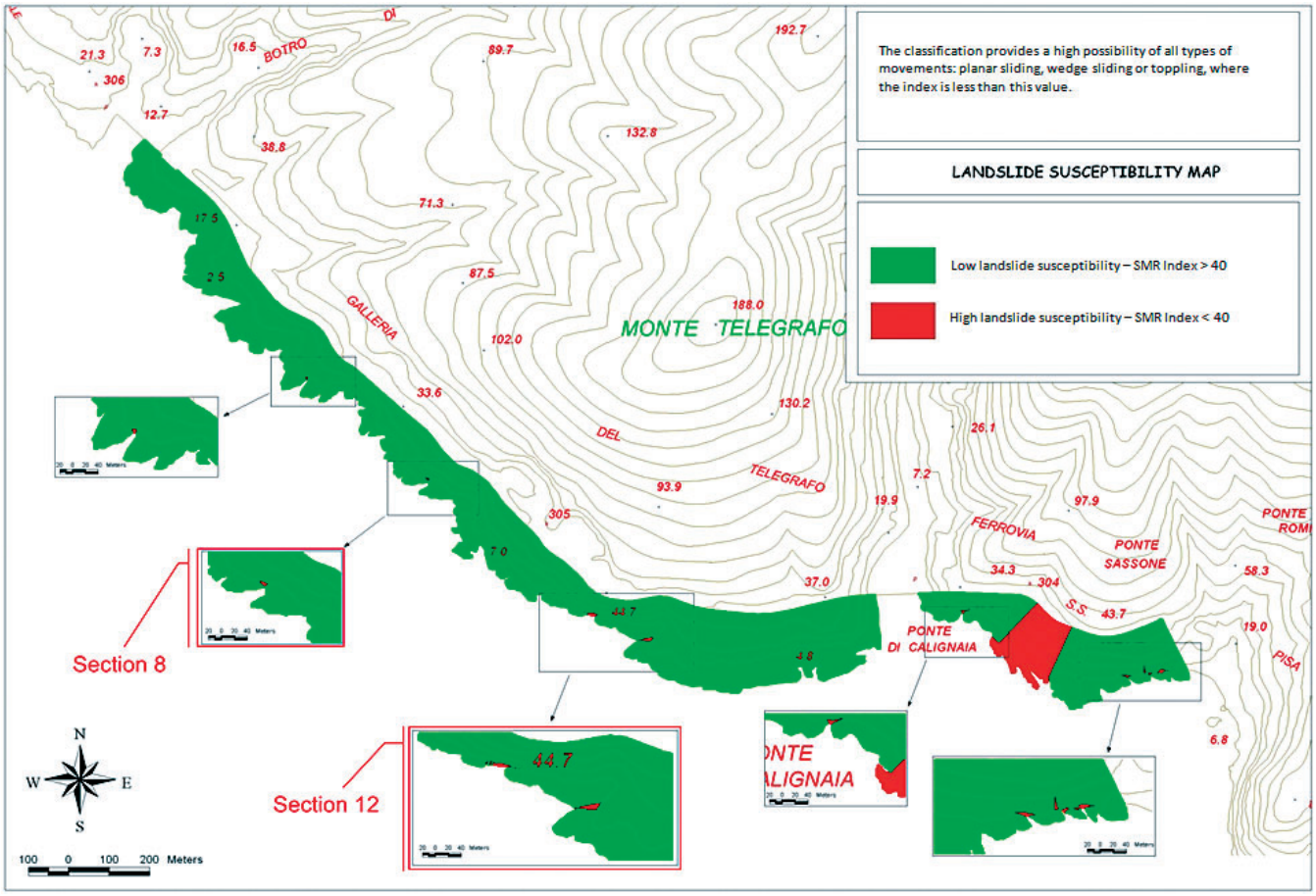

Fig. 10 - Landslide susceptibility map of the coastal area, based on SMR value: the red colour indicates the areas where the SMR index is <40 (higher susceptibility); the green colour the areas where the SMR index is ≥40 (lower susceptibility). The analysis sections (8 and 12) are shown.

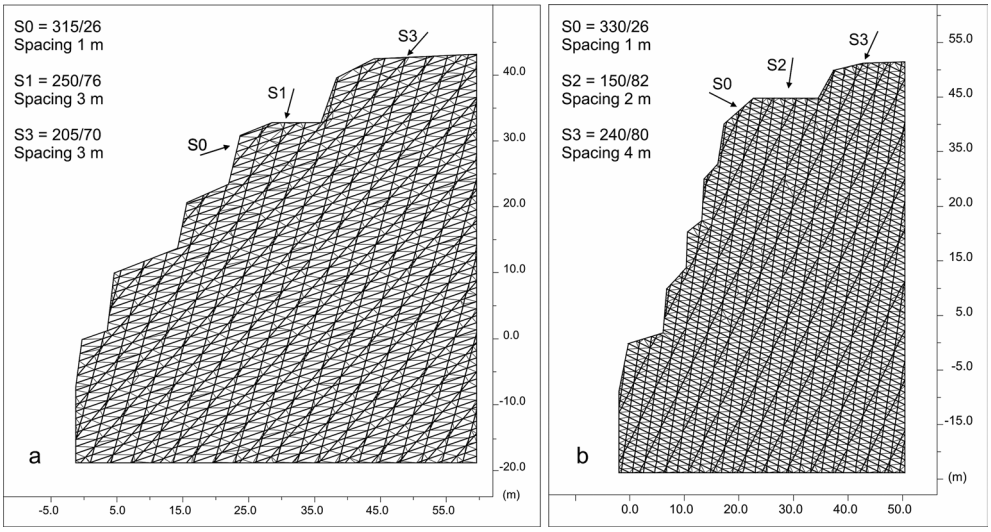

FIG. 11 - Discretization mesh and discontinuities families for the selected sections 8 (a) and 12 (b).

ed to static and dynamic stresses. The mass was discretized in irregular polygons, due to the natural discontinuities: the numerical code permits to analyse their displacements and deformation coupling the motion equations with those of the constitutive laws.

The mass was represented by a set of distinct blocks; discontinuities are considered like boundary of each block; great displacements along the discontinuities and rotations were permitted. UDEC utilizes different constitutive models both for material and the interfaces between the fractures.

From a geological point of view the two selected sections are constituted by the same lithofacies, the sandstone of the Macigno Formation. The discontinuity families, for each section, include the stratification (S0 in fig. 11) and two main joint sets (S1 and S2 in fig.11).

The static and dynamic analyses were carried out by the Hoek and Brown failure criterion (Hoek & *alii* 2002; Marinos & alii 2007) that is expressed by:

$$\sigma_1 = \sigma_3 + \sigma_{ci} (m_b \sigma_3/\sigma_{ci} + s)$$

where σ_1 is the main principal stress, σ_3 is the minus principal stress, m_b, s and a are constants depending on the rock features (density, fracturing degree, plasticity, shear strength, etc.) and σ_{ci} the characteristic compressive strength of the intact rock.

The following four mechanical parameters and three dimensionless constants were utilized:

– unit weight (γ) = 26 kN/m^3
– bulk modulus (K) = 10 GPa
– shear modulus (G) = 5.5 GPa
– σ_c = 41 MPa
– m_b = 2.18
– s = 0.0039

The Mohr-Coulomb criterion was used for the shear strength of the discontinuities, because their properties are functions only of a frictional and cohesive behaviour. In this case the needed parameters are as follows:

– normal stiffness (Jkn) = 1E7 kPa/m
– shear stiffness (Jks) = 1E6 kPa/m;
– friction angle (φ) = 27°;
– cohesion = 220 kPa (for S0, section 8)
– cohesion = 190 kPa (for S0, section 12)
– cohesion = 40 kPa (all the others discontinuities).

All the parameters come from laboratory tests and scientific bibliography.

For both sections static and dynamic analyses were performed. In that regard two real accelerograms have been used whose characteristics are shown in table 1 and fig. 12 (data provided by the Accelerometric Italian Network; RAN, 2006-2007).

For each section, the east-west and north-south accelerometric components were projected along the line of the section and their contributions were added in order to have a single input. The dynamic analysis consists in three different phases: seismic input was applied firstly in the horizontal direction, hence vertically and finally coupled. The third analysis gave the most interesting results, which are shown as follows.

TABLE 1 - Data provided by the Accelerometric Italian Network (RAN, 2006-2007)

Input rec	Date	Station	Lat N (°)	Long E (°)	Epicenter	Lat Epi N (°)	Long Epi E (°)	Epicentral distance (km)	deep (km)	Ml	PGAmax cms-2
AG014	2006.04.17	Livorno	43.500	10.413	northern coast of Tuscany	43.621	10.213	20.99	9.1	3.8	2.525
AI002	2007.08.27	Livorno	43.500	10.413	northern coast of Tuscany	43.503	10.327	6.92	15.3	2.4	3.010

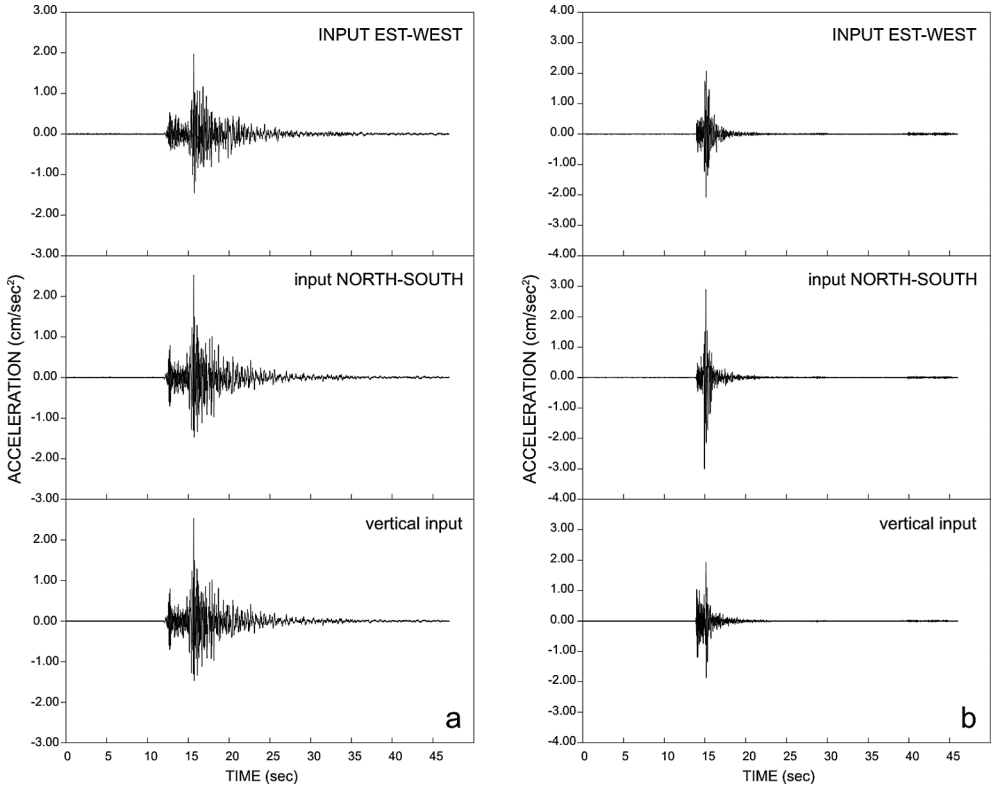

FIG. 12 - Seismic input used in the dynamic analysis (a: AG014; b: AI002).

Section 12

The static analysis shows that the fracture set of the S3 family mostly affects the stability. We know dip and spacing of this family but it is difficult to identify, on the section, the exact points where these fractures emerge. Then we performed some static analysis based on different points of origin of the fracture set. The fracture spacing of the S3 family is approximately 4 m, so we performed analyses by choosing four structural configurations that differ only in the position of passage of the fracture planes located (see fig. 13c) about at the points of coordinates A(0,0), B(1,0), C(2,0) and D(3,0).

In any case all the analysed situations show a general instability of the area. For this section significant displacements were reached with the sets of fractures passing at the points of coordinates B(1,0) and C(2,0).

For the first case the most superficial portion of the slope tends to slide obviously along a fracture belonging to the family S3 (fig. 13); the displacement vectors show low values. In the dynamic analyses it is possible to note a small amplification of the displacements particularly for the AI002 seismic input (fig. 14).

Also in the second case we note a slide of a superficial portion of the slope along a fracture belonging to the S3 family. With this configuration of the fractures the area affected by the movement is much deeper than previous analysis (fig. 15). The toppling of blocks at the base of the slope is clearly visible from the diagram of the deformed grid.

The dynamic analysis showed different results. The area affected by the movement seems to be the same, but the greater displacements are located in the blocks identified by the more superficial fracture belonging to the family S3 (fig. 16).

Section 8

The static analysis shows that the fracture set of greatest importance for the stability is always the S3 set. As done for the section 12, we performed several tests depending on the point of emergence, in this section, of the fracture set whose spacing is 3 m. So we performed analyses by choosing three structural configurations that differ in the position of passage of the fracture planes located about at points (fig. 17c) of coordinates A(0,0), B(1,0), C(2,0). The results show an overall static stability of the slope. For this section significant displacements were reached with the sets of fractures passing at points of coordinates B(1,0) and C(2,0).

In the first case, analysing the diagrams relating to the displacement vectors and the deformed grid for static analysis (fig. 17), the basal part of the section tends to translate along a fracture of the S3 family. The rock detachment in this portion of the slope is placed in correspondence of two fractures belonging to the S1 family.

Dynamic analysis shows different results. In the analysis with the AG014 input the result is similar to the static analysis.

Analysis with AI002 input show largest displacements (fig. 18a) located in a very narrow and shallow zone, lined

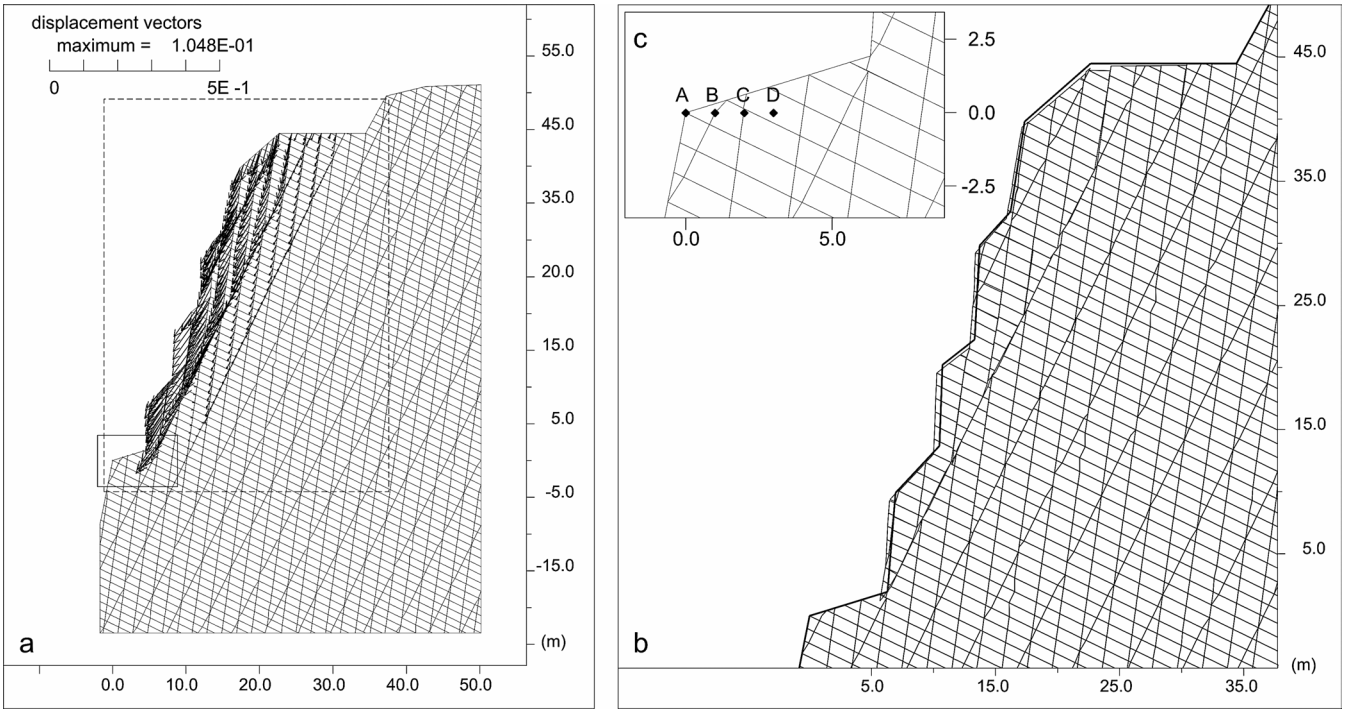

FIG. 13 - Displacements vectors graph (a) and deformed mesh (b) obtained in the static analysis; (c) points of passage of the fracture set.

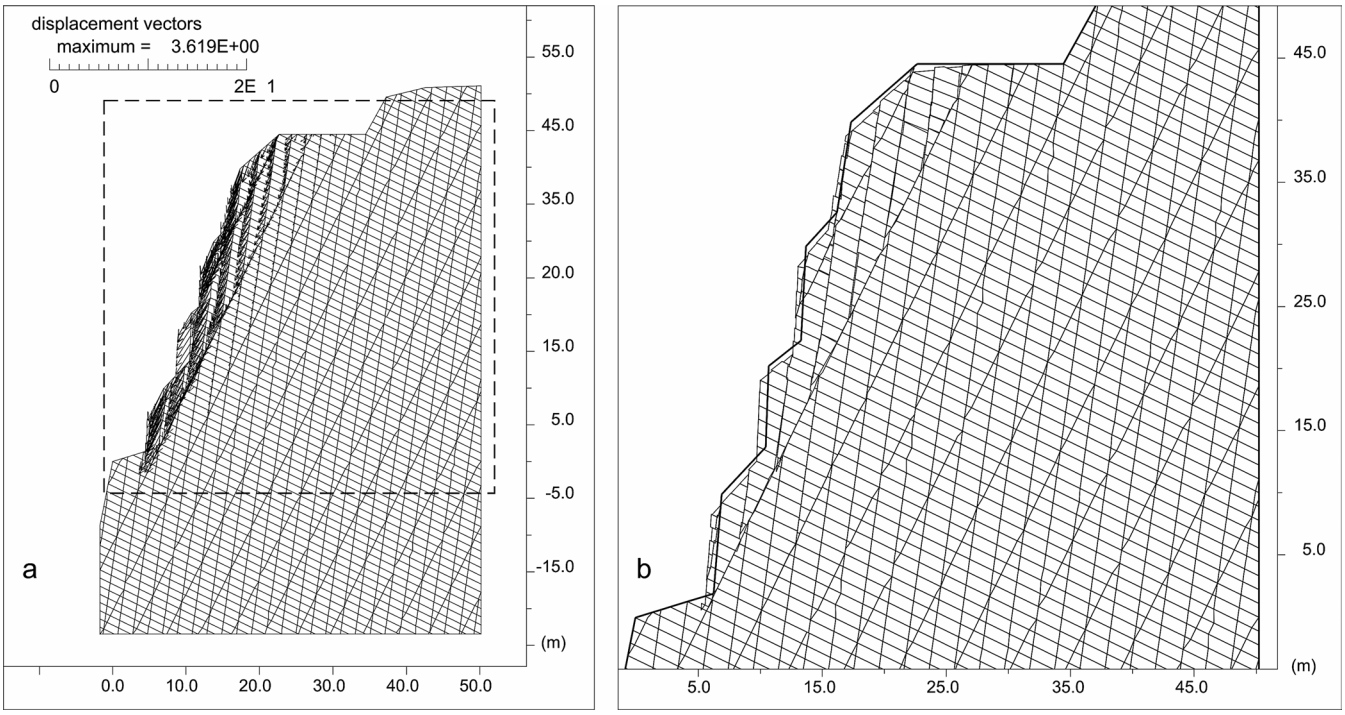

FIG. 14 - Results of dynamic analyses: displacements vectors graph (a) and deformed mesh (b) related to the AI002 seismic input.

with a fracture of the S1 family; also we can see from the deformed grid (fig. 18b) that the blocks affected by the movement tend to topple.

In the second case, analysing the diagrams relating to the displacement vectors and the deformed grid, the static analysis (fig. 19) reveals that the outer zones of the

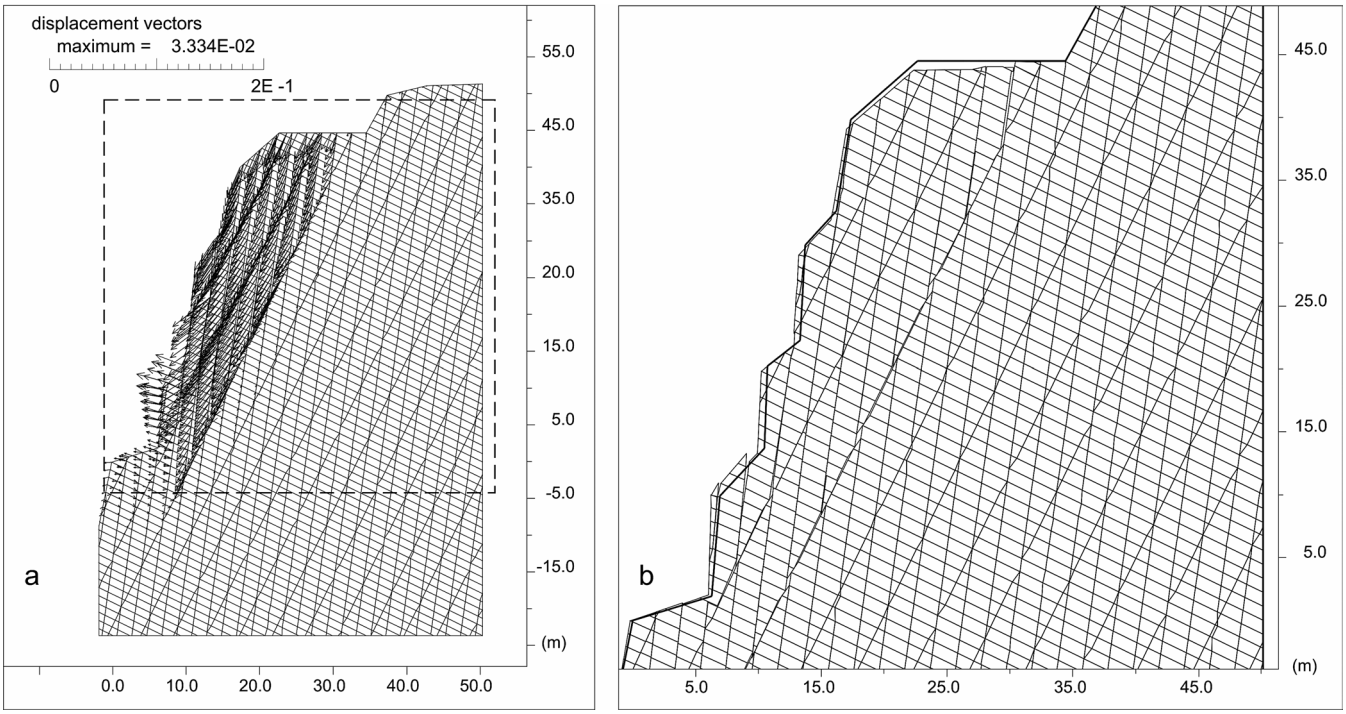

FIG. 15 - Displacements vectors graph (a) and deformed mesh (b) obtained in the static analysis.

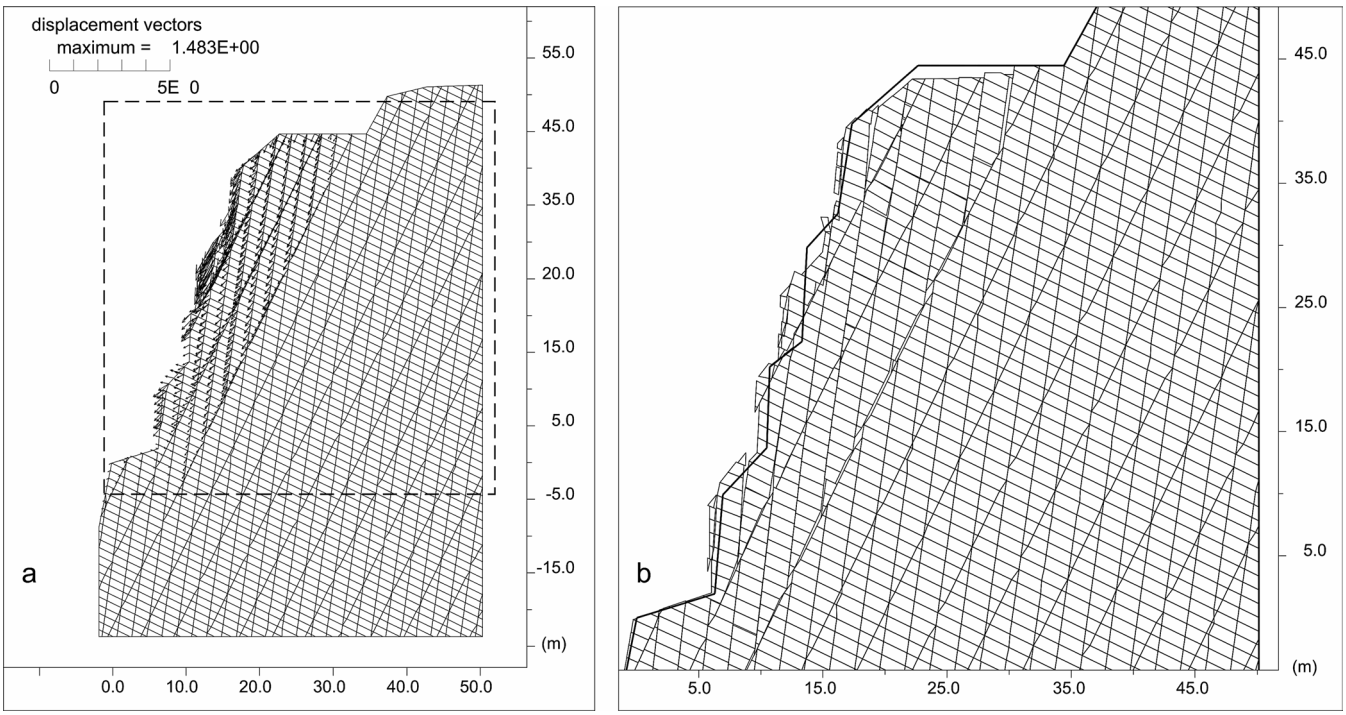

FIG. 16 - Results of dynamic analyses: displacements vectors graph (a) and deformed mesh (b) related to the AI002 seismic input.

slope tend to fall off along the S1 fracture family and to slip along the S3 fracture family. The section is stable, noting also the small size of the maximum displacement vector.

The dynamic analyses (fig. 20) showed a similar pattern of displacement vectors. The largest displacements are localized in a very narrow and shallow zone, bounded by a fracture of the S1 family.

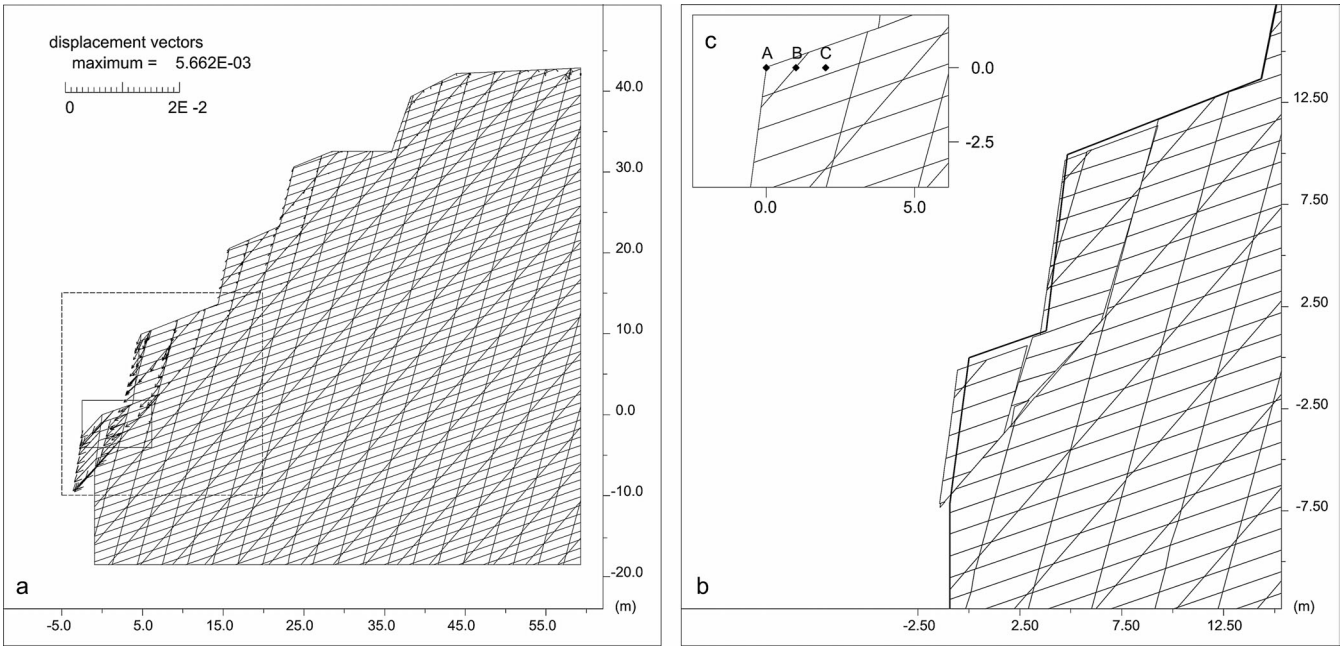

FIG. 17 - Displacements vectors graph (a) and deformed mesh (b) obtained in the static analysis; (c) points of passage of the fracture set.

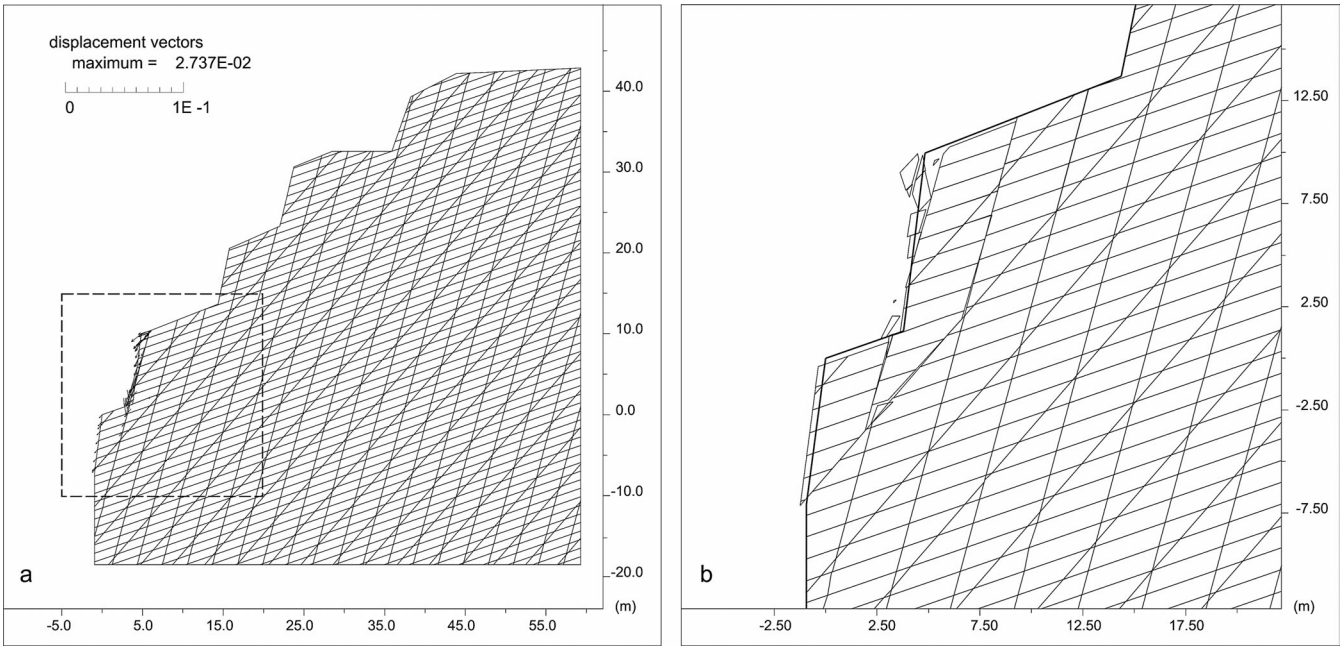

FIG. 18 - Results of dynamic analyses: displacements vectors graph (a) and deformed mesh (b) related the AI002 seismic input.

ROCKFALL SIMULATION

A detailed topographic profile (scale 1:2,000) has been realized for both sections (8 and 12), also taking into consideration the observed attitudes. There are very steep portions of the slope on this sections, due to joints with high dip values (for example the C family - 250/80) but also there are some areas with much lower dips, coinciding with bedding layers (for example the A family - 320/24).

Several parameters govern the boulder motion along a slope and sometimes it is difficult to express them numerically. The trajectories of the blocks depend on the cliff geometry, on the block shape and on the block initial speed. After the first impact with the ground, the restitu-

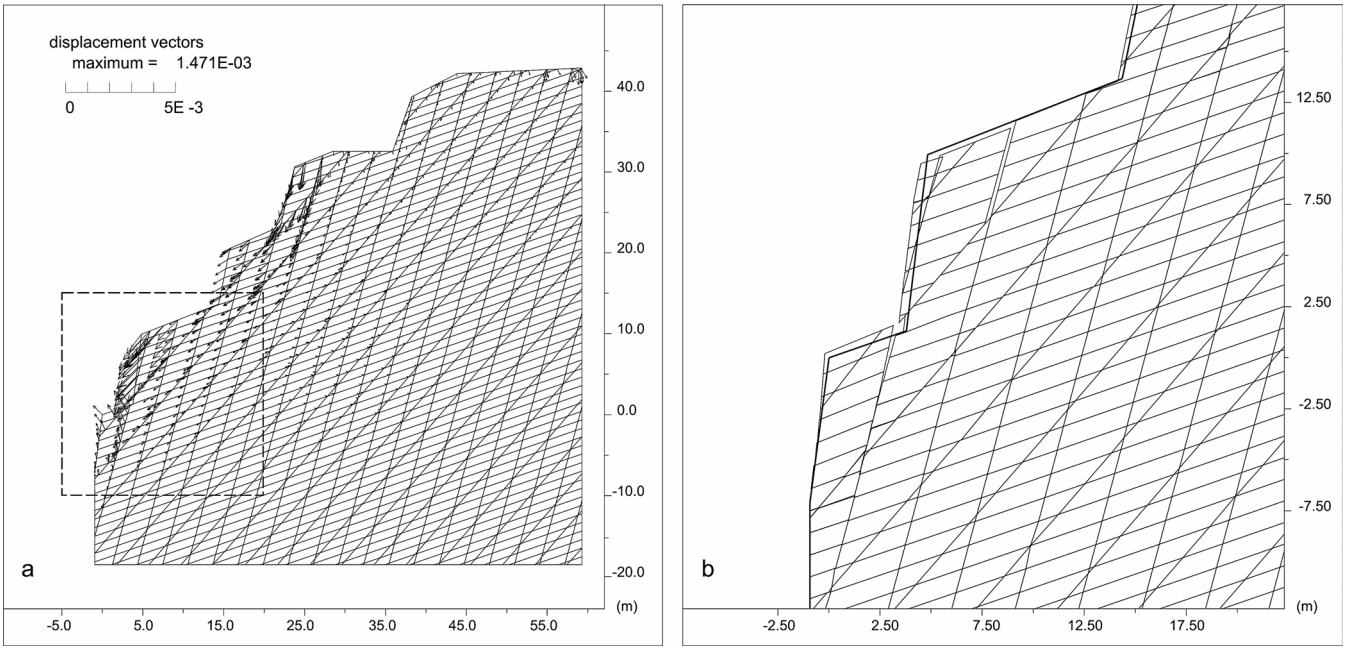

FIG. 19 - Displacements vectors graph (a) and deformed mesh (b) obtained in the static analysis.

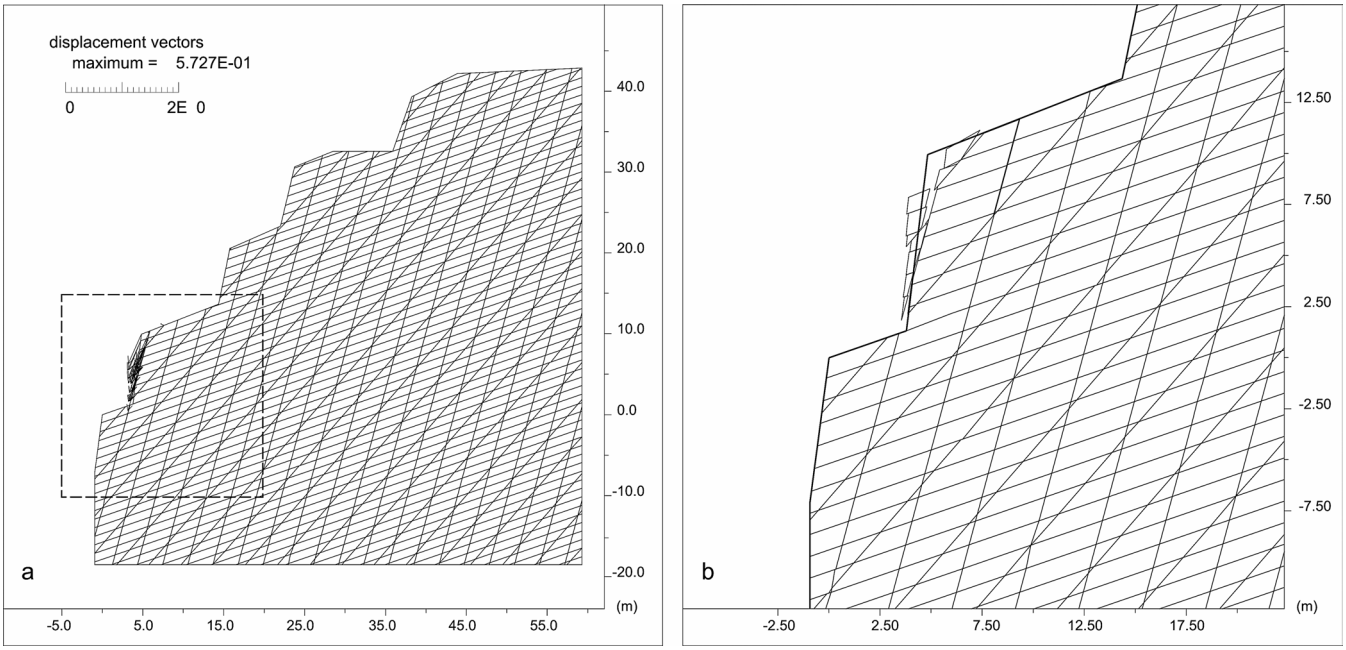

FIG. 20 - Results of dynamic analyses: displacements vectors graph (a) and deformed mesh (b) related to the AG014 seismic input.

tion coefficients (ranging from 0 to 1) express the amount of energy that is returned after each impact. The energy dissipated after each impact is a function of the characteristics of motion along a certain path, the material that constitutes the slope, the mechanical properties of the block and the materials along the slope. In fact it is impossible to model a slope's profile exactly or to determine forms and dimensions of the blocks that can slide along a slope: they are parameters that suffer from variations during the time. It is also difficult to predict the motion of blocks that break during the fall, and it is not even possible to determine in which areas they will break. It's therefore appropriate to refer to simplified models in the simulation software (Rocfall - RocScience).

Some fall simulations were carried out through two different methods, to make a back analysis of previous events and to obtain a more general outline of possible movements. The first, called Lumped mass, is a deterministic method that operates by solving a system of equations that considers the block as a material point on a slope. The second method, called CRSP (Colorado Rockfall Simulation Program, Pfeiffer & Bowen 1989), is a statistical method that provides a series of velocities and bounce heights as a function of input parameters; it uses the real size of the analysed block.

In both cases a set of throw zones (and not a single detachment point on the slope) was chosen: twenty points for the station 8 and fifteen for the station 12. By comparing the results obtained with the two methods, it was noted that the CRSP method provides more realistic models, because it considers the real block size and applies the law of conservation of the total energy. The restitution coefficients have been derived from Pfeiffer & Bowen (1989).

Thanks to the measures recorded during the geomechanical surveys, it was possible to estimate the maximum and minimum block size; the simulations were performed using these different sizes.

Station 8

The blocks were considered as cylinders whose maximum size has got a diameter of 1.25 m and a height of 0.5 m, while the minimum size corresponds to a diameter of 0.25 m and a height of 0.5 m. The characteristics of volume weight and elastic modulus of the Macigno Sandstone Fm. were drawn from laboratory tests and literature.

The velocity components during the detachment were set to rather low values (0.5 m/s) as to assume a fall simply

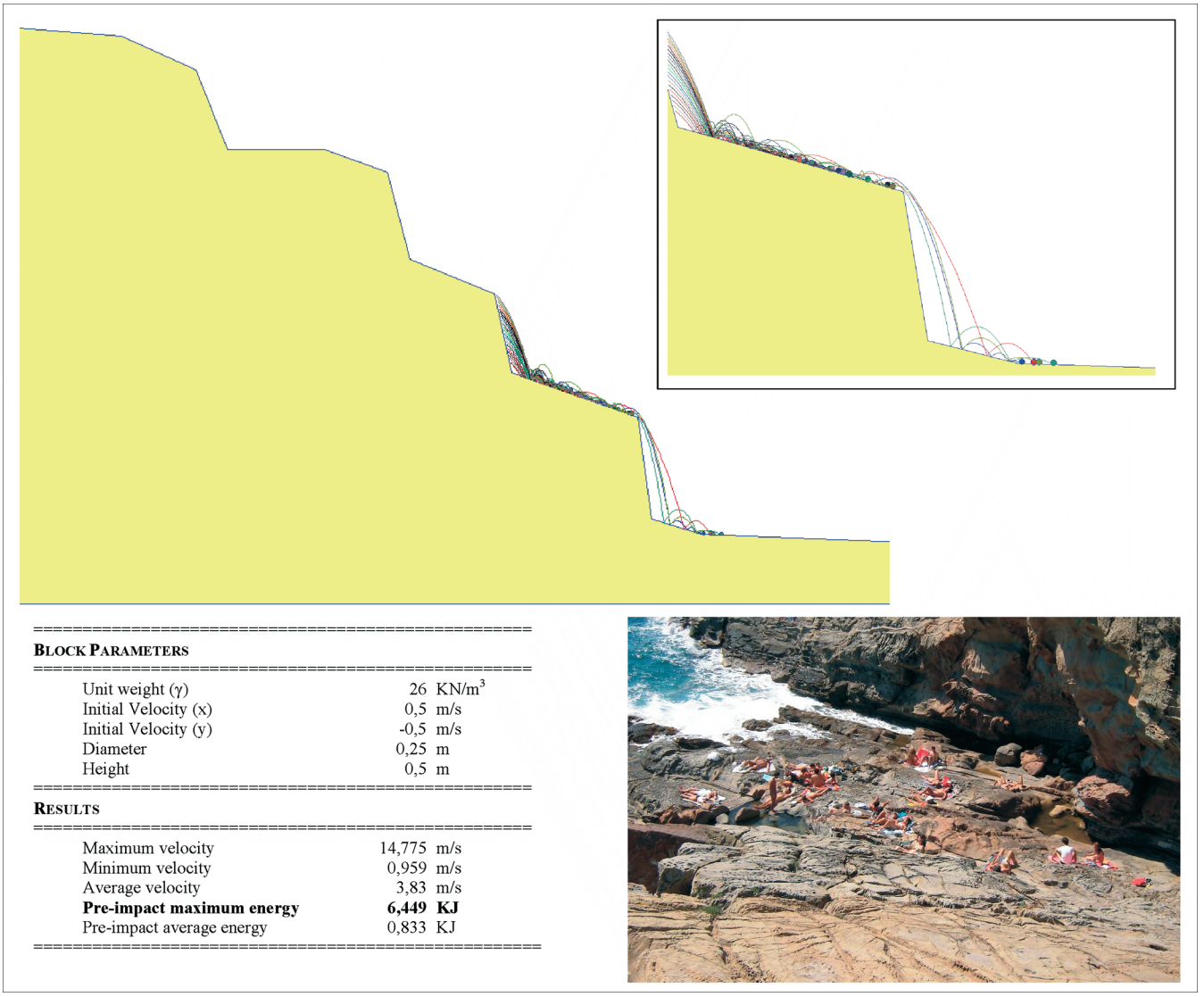

BLOCK PARAMETERS

Unit weight (γ)	26	KN/m^3
Initial Velocity (x)	0,5	m/s
Initial Velocity (y)	-0,5	m/s
Diameter	0,25	m
Height	0,5	m

RESULTS

Maximum velocity	14,775	m/s
Minimum velocity	0,959	m/s
Average velocity	3,83	m/s
Pre-impact maximum energy	**6,449**	**KJ**
Pre-impact average energy	0,833	KJ

FIG. 21 - Rock fall path simulation - Station 8 - Maximum block size.

caused by gravity. In the case of maximum size of the blocks, fifteen of the twenty throws correspond to boulders whose trajectory intercepts the area of stay of the elements at risk (fig. 21). In the simulation for minimum size blocks, only four of the twenty trajectories were considered critical (fig. 22).

Station 12

In this simulations the project mass was also considered as a cylinder, whose dimensions range from 0.25 m in diameter and 0.5 m in height, to 2 m in diameter and 6 m in height; the volume weight and the elastic modulus are considered as constants, as well as the velocity's components during the detachment. By observing the trajectories corresponding to fifteen throws, both for the minimum and maximum size, it is clear that all of them reach the critical risk area (figs. 23 and 24).

The results of the simulations are expressed in the pictures through a simplified scheme, in which the trajectories corresponding to the different throws are represented; the stop points of the blocks can also be observed: several blocks can impact the areas frequented by bathers.

DISCUSSION AND CONCLUSION

The performed study examined a sandstone cliff south of the town of Livorno, between the mouth of the Rio Maroccone to the north and the Cala del Leone to the south, in its most dangerous area, between the sea and the main road Aurelia. The aim was to divide the area in homogeneous hazard classes and assess the pos-

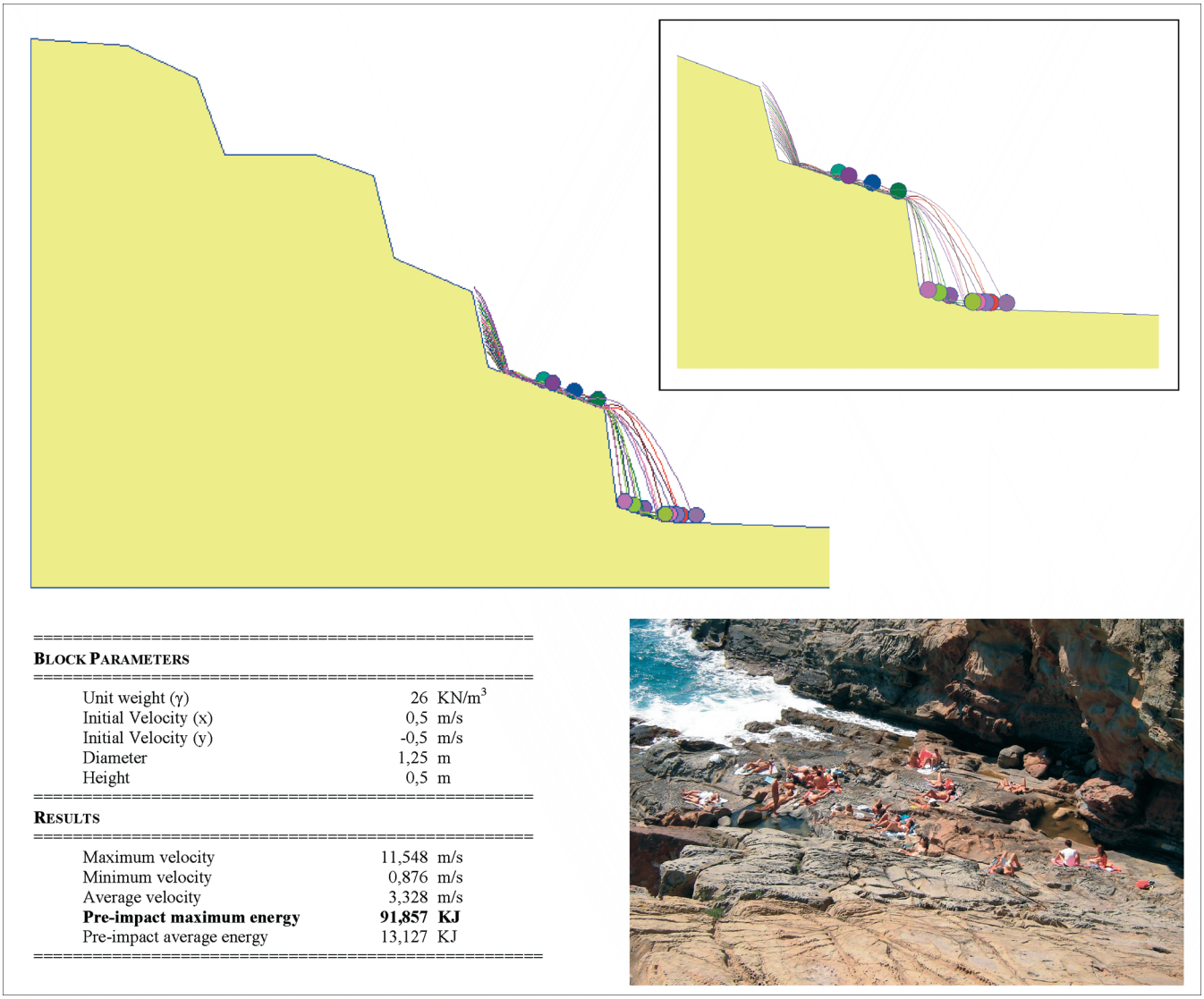

FIG. 22 - Rock fall path simulation - Station 8 - Minimum block size.

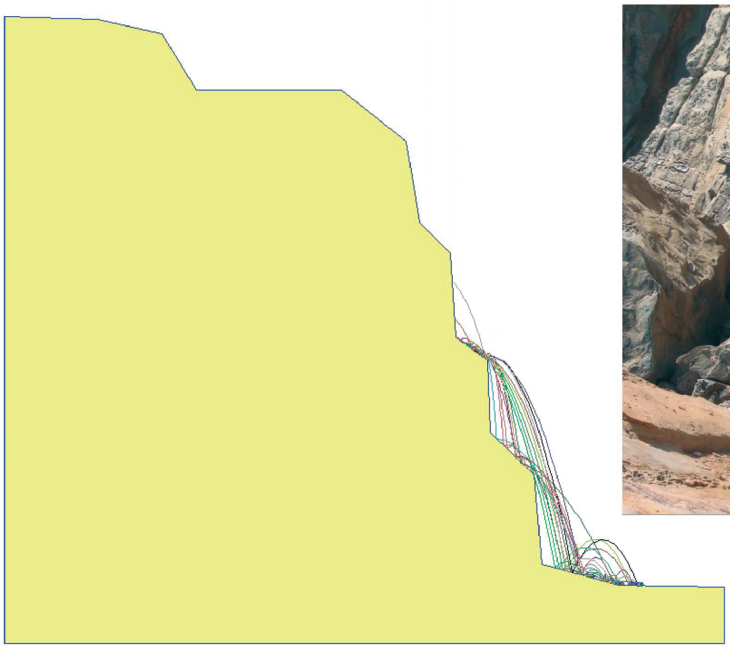

BLOCK PARAMETERS

Unit weight (γ)	26	KN/m^3
Initial Velocity (x)	0,5	m/s
Initial Velocity (y)	-0,5	m/s
Diameter	0,25	m
Height	0,5	m

RESULTS

Maximum velocity	20,095	m/s
Minimum velocity	1,555	m/s
Average velocity	8,042	m/s
Pre-impact maximum energy	**11,411**	**KJ**
Pre-impact average energy	3,059	KJ

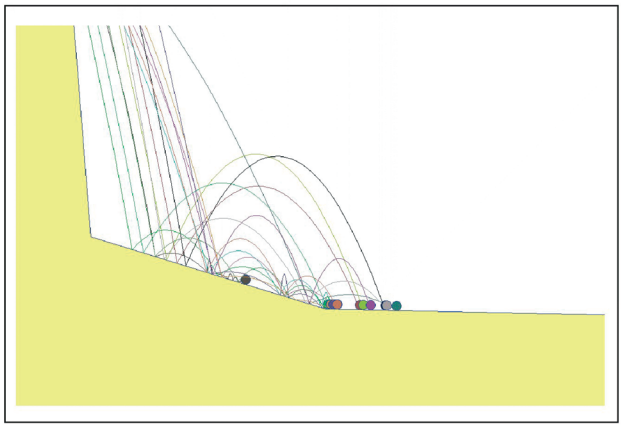

FIG. 23 - Rock fall path simulation - Station 12 - Maximum block size.

sible kinematic evolution. The study refers to an evaluation of parameters that may trigger rock falls on the cliff that could constitute dangers for tourists. The identification of critical areas has been achieved through the elaboration of landslide susceptibility maps. The geotechnical study was carried out on the Macigno Fm. at the site. Field surveys and indirect tests for classifying the rock masses and estimating the uniaxial compression compressive strength (UCS) were performed. Some numerical analyses were executed to study the static and dynamic behaviour of the slope. The results confirm the vulnerability of the area, demonstrating the dynamic instability on the analysed sections and how precarious is the equilibrium even in static conditions. These analyses, compared with the on site surveys, showed poor properties and in some cases alarming results: some portions of the cliff are close to the limit equilibrium conditions, especially in some areas frequented by tourists and bathers. Through the numerical modelling and the rock fall simulations the critical situation of these slopes becomes even more evident. It is confirmed by some rock falls of small blocks occurred during the geomechanical survey period. To make the situation worse, the whole area is constantly subject to exogenous agents like strong winds and wave action, which favour the deterioration of the mechanical features of the Macigno Sandstone.

The synergy between the adopted different scientific approaches has allowed to classify exhaustively all the hazard problems of the investigated area, testifying as only a specific and interdisciplinary methodology can produce results suitable to be used for the real physical, mechanical and evolutionary characterization of a geological system.

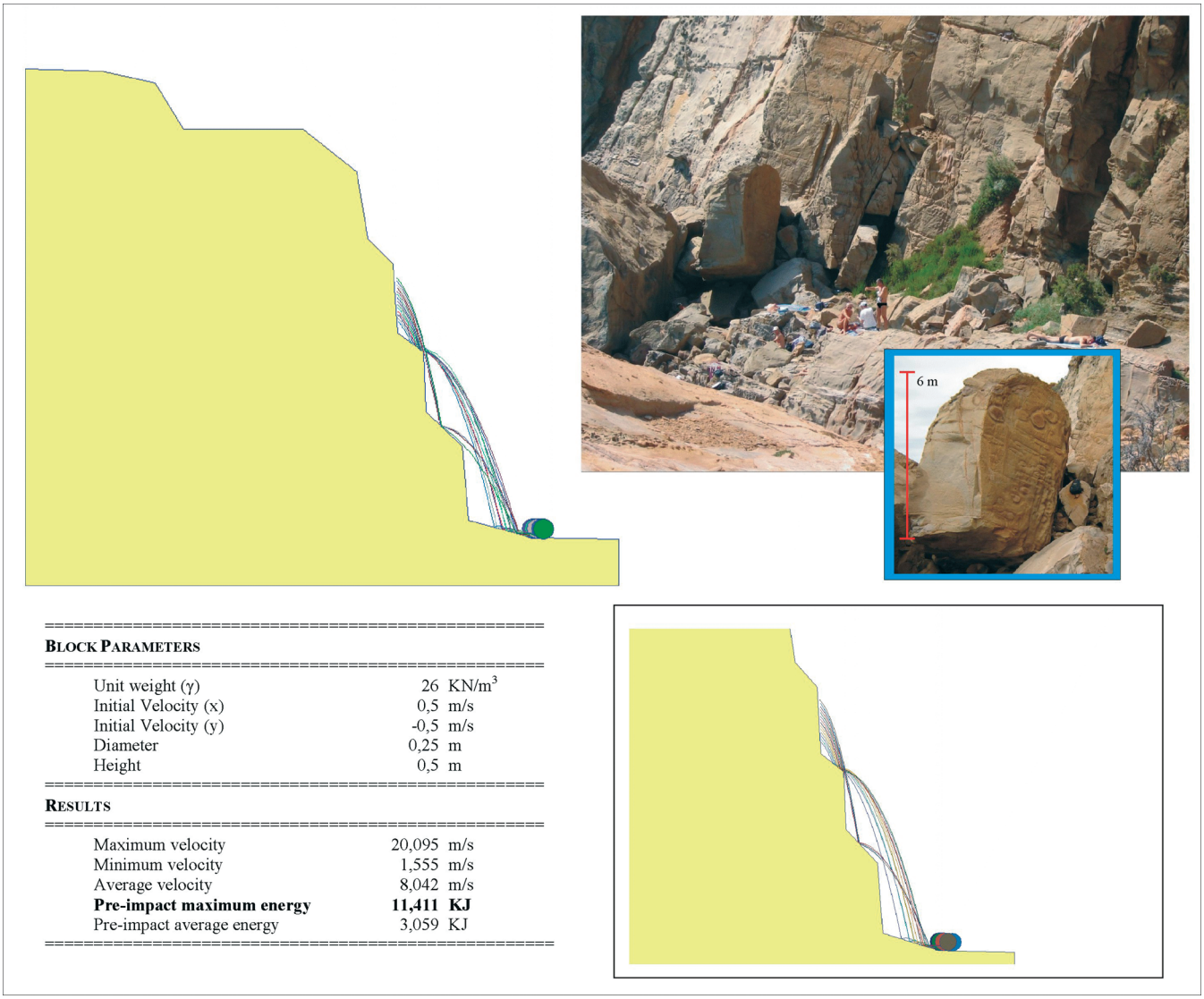

FIG. 24 - Rock fall path simulation - Station 12 - Minimum block size.

REFERENCES

AYDIN A. & Basu A. (2005) - *The Schmidt hammer in rock material characterization*. Engineering Geology, 81, 1-14.

BIENIAWSKI Z.T. (1989) - *Engineering Rock Mass Classifications: a complete manual for engineers and geologists in mining, civil, and petroleum engineering*. Wiley, New York, 251 pp.

BOUMA A.H. (1962) - *Sedimentology of some flysch deposits: a graphic approach to facies interpretation*. Elsevier, Amsterdam, 168 pp..

BROCH E. & FRANKLIN J.A. (1972) - *The Point Load Strength Test*. International Journal of Rock Mechanics and Mining Sciences, 9, 669-697.

CARMIGNANI L. & LAZZAROTTO A. (2004) - *Geological Map of Tuscany (Italy), 1:250,000 scale*. Regione Toscana, Special Edition for the 32nd IGC, Florence, 20-28/8/2004. Tipografia LAC, Firenze.

CONTI P. & LAZZAROTTO A. (2004) - *Geology of Tuscany: evolution of the state-of-knowledge presented by geological maps and the new geological map of Tuscany, 1:250,000 scale*. In: Morini D. & Bruni P. (eds), *The Regione Toscana project of geological mapping*. Special Volume, 32nd IGC, Florence, 20-28/8/2004. Tipografia Martinelli, Firenze, 25-50.

DEERE D.U. & MILLER R.P. (1966) - *Engineering classification and index properties for intact rocks*. Air Force Weapons Laboratory, Technical Report N. AFWL-TR, 65-116, Kirtland Base, New Mexico, pp. 327.

ELTER P., GIGLIA G., TONGIORGI M. & TREVISAN L. (1975) - *Tensional and compressional areas in the recent (Tortonian to present) evolution of the Northern Apennines*. Bollettino di Geofisica Teorica ed Applicata, 17, 3-18.

FENER M., KAHRAMAN S., BILGIL A. & GUNAYDIN O. (2005) - *A comparative evaluation of indirect methods to estimate the compressive strength of rocks*. Rock Mechanics and Rock Engineering, 38 (4), 329-343.

FERRINI G., PANDELI E. & COLI M. (1995) - *Facies e sequenze verticali nel Macigno di Calafuria (Livorno)*. Bollettino della Società Geologica Italiana, 104, 445-458.

GALOPPINI R., MAZZANTI R., TADDEI M., TESSARI R. & VIRESINI R. (1995-96) - *Le cave di arenaria lungo il litorale livornese*. Quaderni del Museo di Storia Naturale di Livorno, 14, 111-146.

FEDERICI P.R. & MAZZANTI R. (1995) - *Note sulle pianure costiere della Toscana*. Memorie della Società Geografica Italiana, 53, 165-270.

HOEK E. & BROWN E.T. (1980) - *Empirical strength criterion for rock masses*. Journal of Geotechnical Engineering Division, ASCE, 106 (GT9), (GT9), 1013-1035.

ISRM (1978) - *Suggested methods for the quantitative description of discontinuities in rock masses*. International Journal of Rock Mechanics, Mining Science and Geomechanics Abstracts, 22, 53-60.

ISRM (1981) - *Rock Characterization, Testing and Monitoring: ISRM suggested methods*. Pergamon Press, pp. 211.

ISRM (1985) - *Suggested methods for determining point-load strength*. International Journal of Rock Mechanics, Mining Science and Geomechanics Abstracts, 22, 53-60.

KATZ O., RECHES Z. & ROEGIERS J.C. (2000) - *Evaluation of mechanical rock properties using a Schmidt hammer*. International Journal of Rock Mechanics, Mining Science and Geomechanics Abstracts, 37, 723-728.

LAZZAROTTO A., MAZZANTI R. & Nencini C. (1990) - *Geologia e morfologia dei Comuni di Livorno e Collesalvetti (with 1:25000 geological map)*. Quaderni del Museo di Storia Naturale di Livorno, 11, Suppl. 2, 1-85.

MARCHETTI D., D'AMATO AVANZI G., SCIARRA N. & CALISTA M. (2008) - *Slope stability modelling of a sandstone cliff south of Livorno (Tuscany, Italy).* Proc. VI International Conference in Computer Simulation Risk Analysis and Hazard Mitigation, Cephalonia, Greece, 5-7/05/2008. WIT Transactions on Information and Communication, 39, 321-333.

MARINOS P.G., MARINOS V. & HOEK E. (2007) - The Geological Strength Index (GSI): a Characterization Tool For Assessing Engineering Properties For Rock Masses. International Workshop on Rock Mass Classification in Underground Mining. Vancouver, 31/5/2007, 87-94.

PANDELI E., FERRINI G. & LAZZERI D. (1994) - *Lithofacies and petrography of the Macigno formation from the Abetone to the Monti del Chianti areas (Northern Apennines).* Memorie della Società Geologica Italiana, 48, 321-329.

PFEIFFER T.J. & BOWEN T. (1989) - *Computer simulation of rockfall*. Bulletin of the International Association of Engineering Geologists, 26 (1), 135-146.

RAN (2006-2007) - http://www.protezionecivile.gov.it/jcms/it/ran.wp

REGIONE TOSCANA - SEISMIC RISK - http://www.rete.toscana.it/sett/pta/sismica/

ROMANA M. (1985) - *New adjustment ratings for application of Bieniawski classification to slopes*. In: International Symposium on the Role of Rock Mechanics, ISRM, Zacatecas, 49-53.

ROMANA M. (1993) - *A geomechanical classification for slopes: slope mass rating*. In: Hudson J.A. (ed): *Comprehensive rock engineering*, Vol. 3, Pergamon, 575-600.

YASAR E. & ERDOGAN Y. (2004) - *Estimation of rock physicomechanical properties using hardness methods*. Engineering Geology, 71, 281-288.

UDEC 4.0 (2004) - Itasca Consulting Group, Inc. Minneapolis, USA.

(Ms. received 1 October 2013; accepted 15 July 2014)